

# Three-dimensional numerical study of converging flux events

J. Dreher<sup>1</sup>, G.T. Birk<sup>2</sup>, and T. Neukirch<sup>3</sup>

<sup>1</sup> Theoretische Physik IV, Ruhr-Universität Bochum, D-44780 Bochum, Germany

<sup>2</sup> Institut für Astronomie und Astrophysik, Ludwig-Maximilians-Universität München, D-81679 München, Germany

<sup>3</sup> School of Mathematical and Computational Sciences, University of St. Andrews, St. Andrews KY16 9SS, Fife, Scotland, UK

Received 30 May 1996 / Accepted 30 July 1996

**Abstract.** The first self-consistent three-dimensional magneto-hydrodynamical simulations of converging magnetic flux events associated with the formation of coronal X-ray bright points are presented. The initial magnetic field results from two magnetic dipoles located below the photosphere at positions  $r_1$  and  $r_2$ , respectively, and an additional horizontal magnetic field parallel to the line  $\overline{r_1 r_2}$ . Both dipole moments are vertical and have equal magnitude but opposite orientation. During the dynamical evolution, a prescribed photospheric convection pattern causes the magnetic dipole-like structures to approach one another. In the early phase of the evolution a current sheet forms in the central region above the polarity inversion line. When the current density exceeds a critical value, anomalous resistivity due to microturbulence is assumed to break the ideal Ohm's law. As a consequence, magnetic reconnection sets in and results in a jet-like plasma flow. The localized plasma heating associated with the reconnection process might account for the flaring of tiny filaments within bright point structures.

**Key words:** solar corona – X-ray bright points – solar magnetic fields – MHD simulations – plasmas

---

## 1. Introduction

X-ray bright points are observed in the solar corona above pairs of opposite polarity magnetic fragments (Vaiana et al. 1970; Golub et al. 1974, 1977; Shibata et al. 1992; Harvey et al. 1994). The observations indicate that a large fraction of these X-ray phenomena are either associated with emerging flux ( $\simeq 1/3$ ) or with cancelling magnetic features ( $\simeq 2/3$ ) (Harvey 1984; Martin 1990a,b). Besides more or less stationary and diffuse soft X-ray emission, bright points often show transient flaring on short time scales (Golub et al. 1974; Strong et al. 1992; Van Driel-Gesztelyi et al. 1996).

*Send offprint requests to:* J. Dreher

The emerging flux model (Heyvarts et al. 1977) has been applied to bright points by Parnell & Priest (1995), and two-dimensional numerical simulations of this model have been carried out by Forbes & Priest (1984) and Yokoyama & Shibata (1995).

Cancelling magnetic features are characterized by magnetic fragments of opposite polarity approaching each other as a result of converging photospheric plasma motion. Recently, a qualitative analytical converging flux model has been put forward that describes various aspects of cancelling magnetic features and their accompanying X-ray bright points (Priest et al. 1994; Parnell et al. 1994a,b). In this model the interacting magnetic fragments are described by means of potential fields. It is assumed that while the fragments approach each other, magnetic reconnection locally occurs and heats the plasma in the reconnection region giving rise to enhanced X-ray emission. Finally, the reconnection leads to the cancellation of the magnetic flux. This model has been very successful in explaining many properties of X-ray bright points associated with cancelling magnetic features.

However, since this model is based on the quasistatic theory and is restricted to potential fields, it does not take into account plasma dynamics and therefore describes some dynamical aspects, e.g. the reconnection process itself, only qualitatively. In order to arrive at a more realistic model, the use of numerical simulations which are not restricted to the above mentioned simplifications seems to be appropriate. As a first step towards this, Rickard & Priest (1994) carried out two-dimensional numerical simulations on the dynamical evolution of magnetic fragments of opposite polarity which are pushed together by converging photospheric flows. These simulations strengthen the view that magnetic reconnection plays an important role in the formation of coronal X-ray bright points. So far, however, a fully three-dimensional self-consistent simulation of converging magnetic flux events has not been carried out.

In this contribution we present results of time-dependent magnetohydrodynamical (MHD) simulations carried out to model the dynamical evolution of approaching magnetic flux fragments in three-dimensional configurations. As an initial

configuration we use two dipole-like magnetic field structures that can be regarded as previously emerged, and a homogeneous horizontal magnetic field. We study the dynamics of the flux converging event caused by prescribed photospheric plasma motion and discuss the relation of the reconnection plasma flow to the observed jet-like outflow from X-ray bright points.

In the next section, we introduce our numerical model while the simulation results are presented in Sect. 3. Finally, we sum up and discuss our findings in Sect. 4.

## 2. The numerical model

The coronal plasma dynamics is modeled by time-integrating the compressible MHD equations (cf. Krall & Trivelpiece, 1986):

$$\begin{aligned} \frac{\partial \rho}{\partial t} + \nabla \cdot (\rho \mathbf{v}) &= 0 & (1) \\ \frac{\partial(\rho \mathbf{v})}{\partial t} + \nabla \cdot (\rho \mathbf{v} \mathbf{v}) &= -\nabla p + \mathbf{j} \times \mathbf{B} & (2) \\ \frac{\partial p}{\partial t} + \nabla \cdot (p \mathbf{v}) &= \frac{2}{3}(-p \nabla \cdot \mathbf{v} + \eta j^2) & (3) \\ \mathbf{E} + \mathbf{v} \times \mathbf{B} &= \eta \mathbf{j} & (4) \\ \frac{\partial \mathbf{B}}{\partial t} &= -\nabla \times \mathbf{E} & (5) \\ \nabla \times \mathbf{B} &= \mu_0 \mathbf{j} & (6) \\ \nabla \cdot \mathbf{B} &= 0 & (7) \end{aligned}$$

Here,  $\rho$ ,  $\mathbf{v}$ , and  $p$  denote the plasma mass density, bulk velocity, and thermal pressure, respectively, while  $\mathbf{B}$ ,  $\mathbf{E}$ ,  $\mathbf{j}$ , and  $\eta$  are the magnetic and electric field, the current density, and the electric resistivity. As usually,  $\mu_0$  denotes the vacuum permittivity. We take into account the heating effects of plasma compressibility and Ohmic dissipation ( $\eta j^2$ ) in the energy equation (3) and include a resistive term ( $\eta \mathbf{j}$ ) in Ohm's law (4).

Time integration of the basic equations (1)–(7) is performed by means of a leapfrog-scheme in a numerical box that covers the domain  $x \in [0, 10]$ ,  $y \in [0, 10]$ ,  $z \in [0, 10]$  and which is resolved by 45 grid points in each direction. The two interacting magnetic fragments are assumed to be symmetric about  $z = 0$  (see Fig. 1, upper panel). Thus, we can restrict our computations to the domain  $z > 0$  and model the region  $z < 0$  by the appropriate symmetric/antisymmetric boundary conditions at  $z = 0$ . As the central interaction region between the two flux fragments is located at this plane, we have used a numerical grid which is non-equidistant along  $z$  and has its maximum resolution ( $\Delta z = 0.05$ ) at  $z = 0$ . Additionally, we assume symmetry about  $y = 0$ . The photospheric layer with its convective plasma motion is represented by boundary conditions  $x = 0$ : Here, a plasma velocity field is prescribed in order to convect the foot-points of the magnetic fragments towards the central interaction region:  $\mathbf{v}_{ph} = -0.007 \tanh(z/3) \mathbf{e}_z$  where the normalizing unit is the Alfvén velocity (see below).

Motivated by present models of converging flux events which make use of potential magnetic fields to describe the

two approaching magnetic fragments (e.g., Priest et al., 1994), we chose for our simulations the initial magnetic field as

$$\mathbf{B}(\mathbf{r}) = b \sum_{i=1,2} \left[ \frac{3(\mathbf{r} - \mathbf{r}_i)((\mathbf{r} - \mathbf{r}_i) \cdot \mathbf{m}_i) - (\mathbf{r} - \mathbf{r}_i)^2 \mathbf{m}_i}{|\mathbf{r} - \mathbf{r}_i|^5} \right] + \mathbf{B}_{hom} \quad (8)$$

with  $\mathbf{r}_1 = (-5, 0, 5)$ ,  $\mathbf{r}_2 = (-5, 0, -5)$ ,  $\mathbf{m}_1 = \mathbf{e}_x$ ,  $\mathbf{m}_2 = -\mathbf{e}_x$ ,  $\mathbf{B}_{hom} = 0.1 \mathbf{e}_z$  and  $b = 50$ . This field results from two magnetic dipoles located below the photosphere at  $\mathbf{r}_1$  and  $\mathbf{r}_2$ , respectively, and a homogeneous magnetic field along  $\mathbf{e}_z$ . The dipoles are of equal strength ( $m = 1$ ) but opposite polarity with their magnetic moments being aligned with  $\mathbf{e}_x$ . The scalar factor  $b$  is chosen such that the maximum magnetic field magnitude is of the order of unity in the numerical box. Further, we assume for the initial configuration a homogeneous isothermal low- $\beta$  plasma ( $\beta = p2\mu_0/B^2$ ) with  $p = 0.1$  and  $\rho = 1$  in normalized units.

The normalizing values chosen are motivated by the solar corona context (cf. Priest et al. 1994; Rickard & Priest 1994):  $B_0 = 10^{-2} T$ ,  $n_0 = 10^{15} m^{-3}$ ,  $L_0 = 10^6 m$ . Here,  $B_0$ ,  $n_0$ , and  $L_0$  are typical values of the magnetic field magnitude, the number density, and the characteristic length, respectively. The resulting Alfvén velocity for the electron-proton plasma is  $v_A = 10^7 ms^{-1}$  and the Alfvénic transit time follows as  $\tau_A = 0.1 s$ .

It is to be expected both from analytical considerations and from the previous two-dimensional numerical studies that due to the photospheric convection, the magnetic flux will be piled up around  $z = 0$  and a current sheet will form there. In our simulation, we assume that if the current density exceeds a critical threshold  $j_{crit}$ , current driven microturbulence sets in and gives rise to anomalous resistivity (e.g. Huba 1985; Benz 1993) which in course might lead to magnetic reconnection. To model this scenario, we choose the anomalous resistivity as

$$\eta = \begin{cases} \hat{\eta}(|\mathbf{j}| - j_{crit})^2 & , \text{ if } |\mathbf{j}| \geq j_{crit} \\ 0 & , \text{ else} \end{cases} \quad (9)$$

with  $j_{crit} = 0.3$  and  $\hat{\eta} = 0.15$ . The choice for the resistivity model in (9) is motivated by the fact that the lower-hybrid drift instability can be excited rather easily in reconnection configurations (Huba, 1985). Its onset criterion is roughly given by  $|\mathbf{v}_D| > v_i(m_e/m_i)^{1/4}$  where  $\mathbf{v}_D$  denotes the drift velocity between ions and electrons and  $v_i$ ,  $m_e$  and  $m_i$  are the ion thermal velocity and the electron and ion mass, respectively (Davidson et al., 1977). From particle simulations, the resulting macroscopic resistivity is found to scale as  $v_D^2$  (Brackbill et al., 1984). At this point, we stress that the values of  $j_{crit}$  and  $\hat{\eta}$  that we used in our simulations differ from the estimates that one obtains from the investigation of the lower-hybrid drift instability by several orders of magnitude. The reason for this discrepancy is, of course, the technical limit of a numerical simulation with respect to the resolution of length and time scales. In this sense, the simulations are rather qualitative. However, various simulations with different resistivity models have shown that the choice of a particular model for  $\eta$  in (9) is not crucial to the qualitative results.

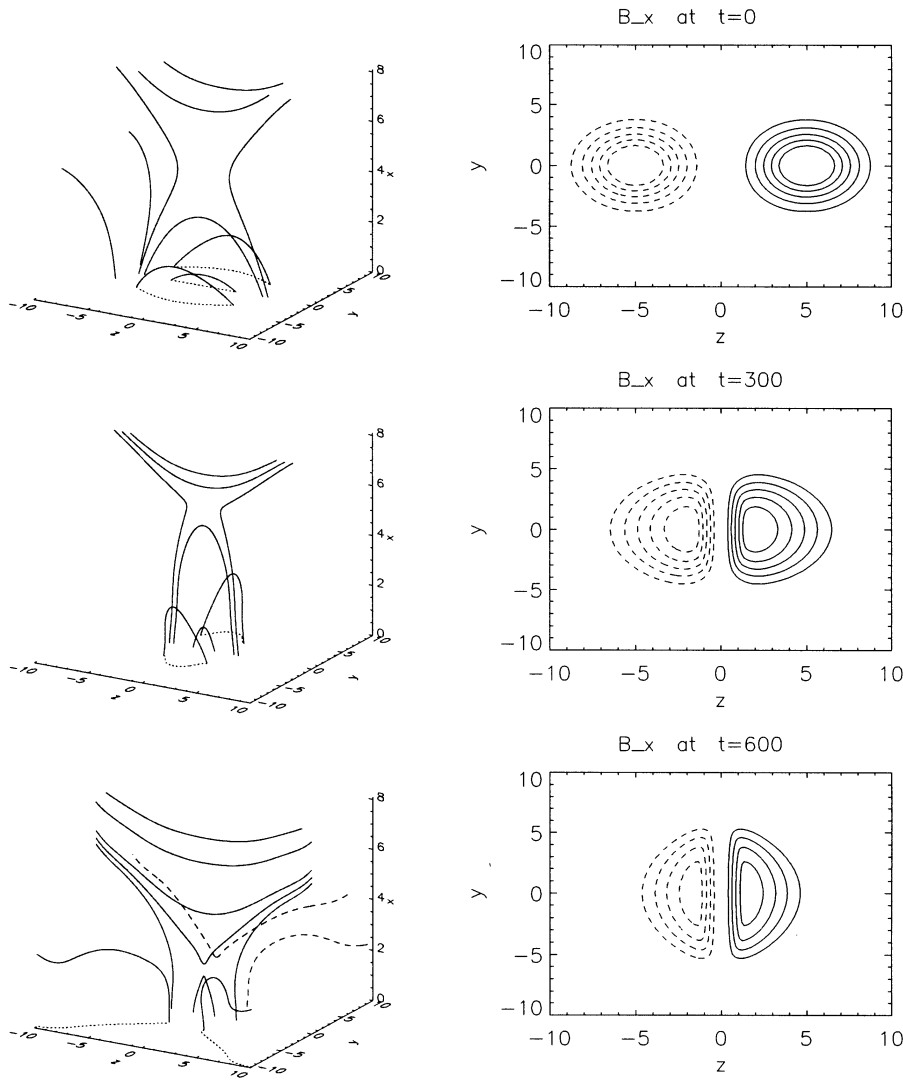


**Fig. 1.** Selected magnetic field lines (left column) and contours of  $B_x$  in the photospheric boundary ( $x = 0$ ) (right column) at  $t = 0$ , 300, and 600. Contour lines are plotted for  $B_x = \pm 0.2, 0.3, 0.4, 0.5, 0.6$

### 3. Simulation results

In the following, we show the results of a simulation in which the dynamical evolution of a converging flux event is followed over a period of 600 Alfvénic transit times. Fig. 1 shows for different times selected magnetic field lines (left column) and contour plots of  $B_x$  in the photospheric boundary, i.e.,  $x = 0$  (right column). The uppermost panel reflects the initial magnetic field: Field lines connecting the two flux fragments, those connecting the fragments with the overlying magnetic field and field lines which represent the latter can readily be identified. Due to the highly symmetric configuration, the magnetic field exhibits an x-line with  $\mathbf{B} = 0$  in the plane  $z = 0$ . This x-line intersects the plane  $y = 0$  at  $x \approx 4.5$  and separates the field lines of different topologies here. In the contour plots of  $B_x$ , the contours at  $z > 0$  represent upward directed flux ( $B_x > 0$ ) while at  $z < 0$ , the flux penetrates into the photosphere. Contour lines are plotted for the values  $\pm 0.2, 0.3, 0.4, 0.5, 0.6$ .

At  $t = 300$ , the flux fragments threading the photosphere have considerably approached the plane of symmetry,  $z = 0$ . As a consequence, the magnetic flux is piled up and the x-

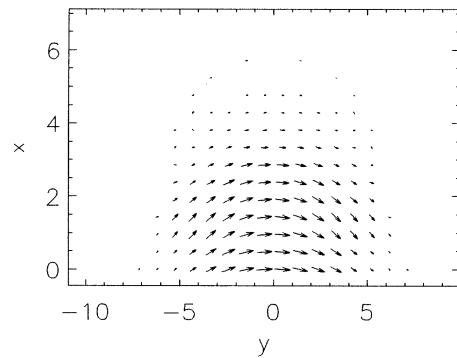


**Fig. 2.** The current density  $\mathbf{j}$  in the plane  $z = 0$ , i.e., between the flux fragments, at  $t = 300$ . The maximum value of  $|\mathbf{j}|$  is 0.5

line has risen. The flux pile-up is associated with the formation of a current system between the flux fragments (cf. Fig. 2). The current density is localized around  $z = 0$ , as can be seen from Fig. 3. As it locally has become supercritical, electrical

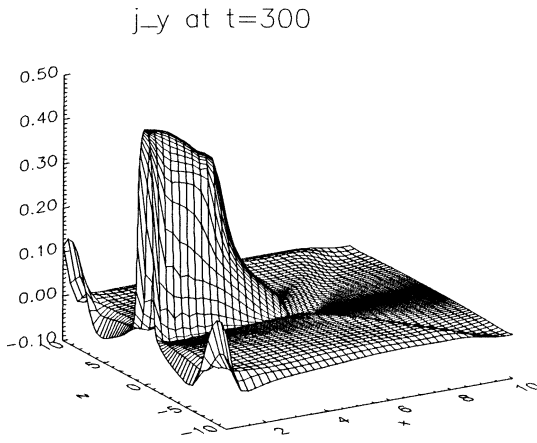


**Fig. 3.** The  $y$ -component of the current density at  $t = 300$  and  $y = 0$

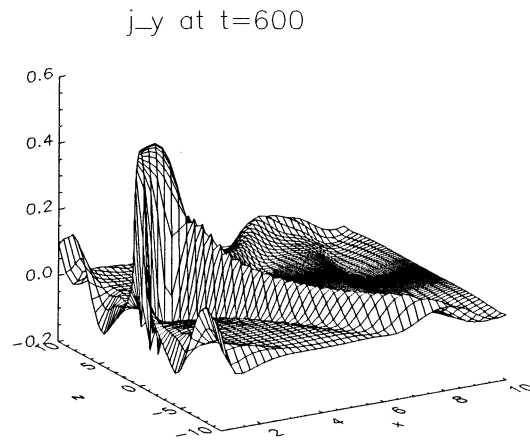


**Fig. 6.** The  $y$ -component of the current density at  $t = 600$  and  $y = 0$

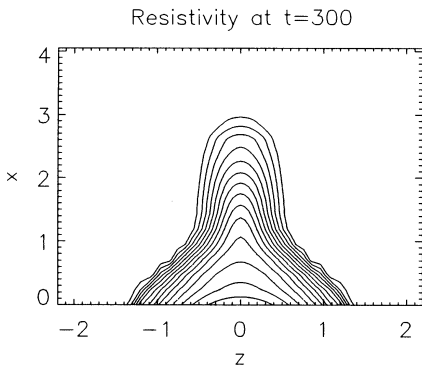


**Fig. 4.** Contour plot of the resistivity at  $t = 300$  and  $y = 0$ . The maximum value is  $6.5 \cdot 10^{-3}$

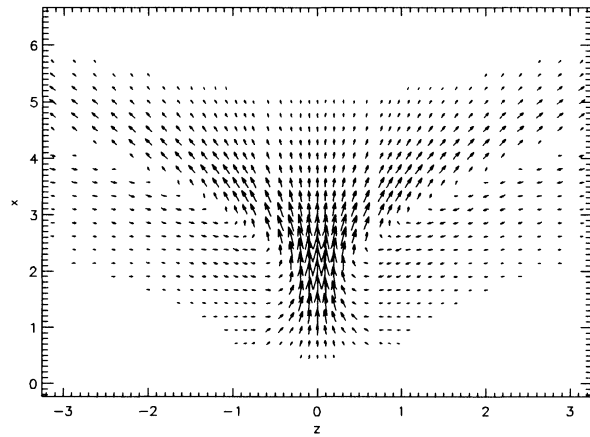


**Fig. 7.** Plasma velocity in the plane  $y = 0$  at  $t = 600$ . The maximum value of  $|v|$  is 0.1

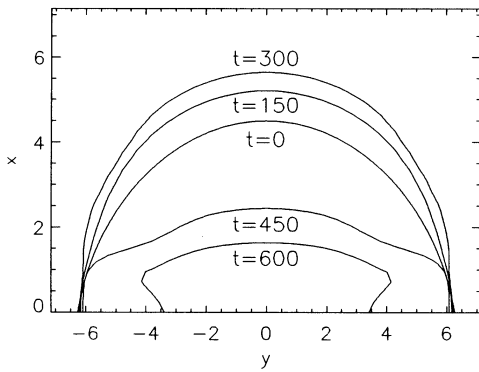


**Fig. 5.** Positions of the  $x$ -line ( $B = 0$ ) in the plane  $z = 0$  at different times

resistivity ( $\eta$ ) has set in. Fig. 4 shows a contour plot of  $\eta$  in the plane  $y = 0$ .

The lower panel of Fig. 1 sketches the magnetic field at  $t = 600$ . Here, magnetic field lines that are located at  $y > 0$  are represented by dashed lines. Due to magnetic reconnection, a certain amount of the magnetic flux has been cancelled. This can easily be seen from the contour plot of  $B_x$ , where the peak magnitudes now are less than 0.6. In comparison to the earlier stages, the intersection of the  $x$ -line with the plane  $y = 0$  has

fallen. A more detailed analysis of the dynamic evolution of the  $x$ -line is given in Fig. 5. Here, the positions of  $B = 0$  in the symmetry plane  $z = 0$  is shown for various times.

Fig. 6 shows the  $y$ -component of the current density at  $t = 600$ . While the maximum value is comparable to the one at  $t = 300$  (cf. Fig. 3), its shape has been altered considerably by the reconnection process: While  $j_y$  decreases sharply with  $x$  in the central plane  $z = 0$ , the formation of shock-like structures which extend from the  $x$ -line along the separatrices can be observed. An additional signature of the reconnection process can be found in the plasma flow velocity (see Fig. 7): Plasma is accelerated upward in the vicinity of the  $x$ -line. The outflow velocity pattern, however, is largely influenced by the shape of the separatrices.

An important aspect in the context of X-ray bright points is the heating associated with the plasma dynamics. In Fig. 8a we show the temperature at  $z = 0$  and  $t = 150$ . At this time, the current density has not yet reached the critical value. Thus, no anomalous resistivity is present, and the observable local increase in temperature of about 30% compared to the initial value ( $T_0 = 0.1$  in normalized units) is solely due to compressional heating. Although this effect still persists at later times, the dras-

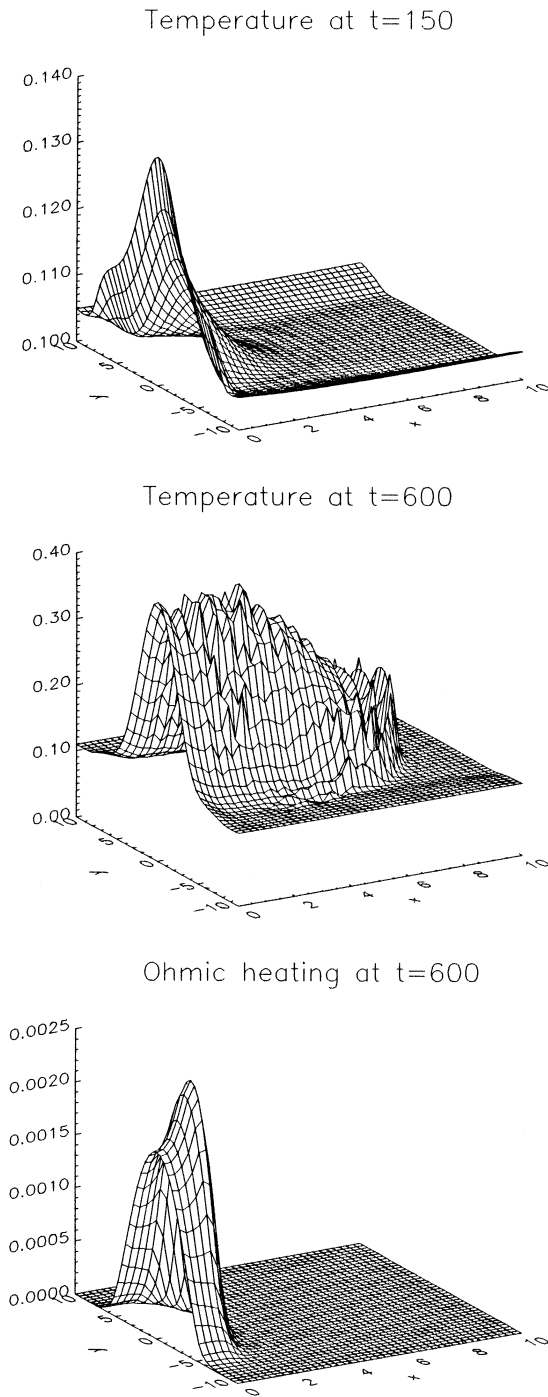


**Fig. 8a–c.** Temperature at  $t = 150$  (a), at  $t = 600$  (b) and the Ohmic heating rate  $\eta j^2$  at this time (c). (Note the different scalings in a and b)

tic temperature increase observable at  $t = 600$  (cf. Fig. 8b) is mainly caused by Ohmic heating. Fig. 8c shows the corresponding heating rate ( $\eta j^2$ ). While the heating is confined to  $x < 2$ , the upward directed plasma motion leads to the formation of a more extended region of comparatively hot plasma.

#### 4. Summary and discussion

In this paper we presented results of three-dimensional time-dependent MHD computations carried out to study the dynamics of converging magnetic flux events. We investigated the evolution of two initially current-free magnetic fragments under the influence of converging photospheric plasma motion. As a first step, we considered a highly symmetric configuration which contains a magnetic null line in the symmetry plane between the flux fragments. We have considered effects which during the evolution might result in the violation of ideal Ohm's law by taking into account a current density dependent resistivity to model the anomalous dissipation caused by microturbulence.

The early quasistatic stage of the simulations is characterized by a moderate heating due to plasma compression as a consequence of the prescribed convergent photospheric motion. As the footpoint motion has been chosen unrealistically high in our simulations in order to make the computation feasible, the significance of this compressional heating might be doubted, in particular when reconsidering the rather simple form of the energy equation (3) which neglects radiation and heat conduction. However, an important and realistic feature of the interaction phase is the storage of free energy in the magnetic field due to the pile-up of magnetic flux and the formation of a current system between the two fragments. As the current density becomes supercritical, the onset of finite resistivity allows for magnetic reconnection and thereby initiates a very dynamic phase. During this phase, magnetic flux is partly cancelled, plasma is accelerated away from the interaction region, and the Ohmic heating associated with the reconnection process leads to a drastic local temperature enhancement.

While magnetic reconnection has previously been proposed to account for heating in X-ray bright points (Priest et al., 1994; Parnell et al., 1994a,b), we are now able to describe the entire evolution of these phenomena within a self-consistent three-dimensional dynamical model without the restriction to potential fields. However, we can corroborate the main ideas of the idealized analytical model introduced by Priest et al. (1994) even in a three-dimensional configuration. In particular, the different stages of the converging flux event can be illustrated by the slow rise of the x-line in the quasistationary phase and its subsequent rapid fall during reconnection (see Fig. 5). Of course, this magnetic null line and its location in the plane  $z = 0$  is a consequence of the symmetry properties of the present model configuration.

A further characteristic signature of magnetic reconnection is the generation of jet-like plasma flow (see Fig. 7). Generally the flow pattern is largely influenced by the magnetic field structure and can be fairly complex in three-dimensional configurations. In fact, such flows are observed in the vicinity of bright points (Shibata et al. 1992).

We note that our numerical investigations should be understood as qualitative studies of converging magnetic flux events rather than giving exact quantitative results. In particular, the magnitudes of the thermal pressure, the electrical resistivity and the the photospheric convection velocity have been chosen on the basis of technical feasibility. Also, a more realistic model might include the effects of heat conduction and radiative energy losses. However, we feel that the agreement of our results with previous idealized analytical predictions on the one hand and with observational key features on the other hand are encouraging for further more detailed studies in this field.

*Acknowledgements.* We thank C. E. Parnell for helpful discussions. This work has been supported by the Deutsche Forschungsgemeinschaft through Sonderforschungsbereich SFB 191, Teilprojekt C2 (JD) and grant ME 745/18-1 (GB) and by the United Kingdom Particle Physics and Astronomy Research Council (TN). We also acknowledge support by the British-German Academic Research Collaboration programme.

## References

- Benz, A. O. 1993, *Plasma Astrophysics*, Kluwer, Dordrecht, p. 223
- Brackbill, J. U., Forslund, D. W., Quest, K. B., Winske, D. 1984, *Phys. Fluids*, 27, 2682
- Davidson, R. C., Gladd, N. T., Wu, C. S. 1977, *Phys. Fluids*, 20, 301
- Forbes, T. G., Priest, E. R. 1984, *Sol. Phys.*, 94, 315
- Golub, L., Krieger, A. S., Silk, J., Timothy, A., Vaiana, G. 1974, *ApJ*, 189, L93
- Golub, L., Krieger, A. S., Harvey, J., Vaiana, G. 1977, *Sol. Phys.*, 53, 111
- Harvey, K. L. 1984, *ESA SP*, 220, 235
- Harvey, K. L., Nitta, N., Strong, K. T., Tsuneta, S. 1994, in *Frontiers Science Series 10*, ed. by Y. Uchida, T. Watanabe, K. Shibata, H. S. Hudson, 21
- Heyvarts, J., Priest, E. R., Rust, D. M. 1977, *ApJ*, 216, 123
- Huba, J. D. 1985, in *Unstable Current Systems and Plasma Instabilities in Astrophysics*, ed. by M. R. Kundu and G. D. Holman, D. Reidel, Dordrecht, p. 315
- Krall, N. A. A. W. Trivelpiece 1986, *Principles of Plasma Physics*, San Francisco Press, San Francisco, p.119
- Martin, S. F. 1990a, *IAU Symp.*, 138, 130
- Martin, S. F. 1990b, *Mem. A. S. It.*, 61, 293
- Parnell, C. E. Priest, E. R. 1995, *Geophys. Astrophys. Fluid Dynamics*, 80, 255
- Parnell, C. E., Priest, E. R., Golub, L. 1994a, *Sol. Phys.*, 151, 57
- Parnell, C. E., Priest, E. R., Titov, V. S. 1994b, *Sol. Phys.*, 153, 217
- Priest, E. R., Parnell, C. E., Martin, S. F. 1994, *ApJ*, 427, 459
- Rickard, J. Priest, E. R. 1994, *Sol. Phys.*, 151, 1
- Shibata, K., Ishido, Y., Acton, L. W., et al. 1992, *PASJ*, 44, L173
- Strong, K., Harvey, K., Hirayama, T., et al. 1992, *PASJ*, 44, L161
- Vaiana, G. S., Krieger, A. S., Van Speybroeck, L. P., Zehnpfennig, T. 1970, *BAAS*, 15, 611
- Van Driel-Gesztelyi, L., Schmieder, B., Cauzzi, et al. 1996, *Sol. Phys.*, 163, 145
- Yokoyama, T. Shibata, K. 1995, *Nature*, 375, 42